

Investigating Domain Gaps for Indoor 3D Object Detection

Zijing Zhao

zijingzhao@stu.pku.edu.cn

Wangxuan Institute of Computer
Technology, Peking University
Beijing, China

Zhu Xu

xuzhu@stu.pku.edu.cn

Wangxuan Institute of Computer
Technology, Peking University
Beijing, China

Qingchao Chen

qingchao.chen@pku.edu.cn

National Institute of Health Data
Science, Peking University
Beijing, China

Yuxin Peng

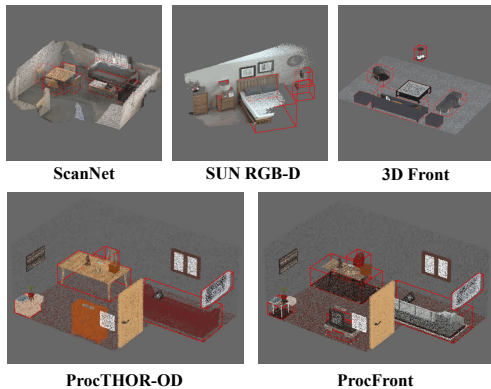
pengyuxin@pku.edu.cn

Wangxuan Institute of Computer
Technology, Peking University
Beijing, China

Yang Liu*

yangliu@pku.edu.cn

Wangxuan Institute of Computer
Technology, Peking University
Beijing, China



(a) Indoor point clouds visualization in different datasets

Figure 1: (a) Point clouds in different datasets exhibit significant differences in point cloud quality, bounding box layout and object features. (b) mAP within and across datasets. The performance shows a drastic decline in cross-dataset evaluation.

ABSTRACT

As a fundamental task for indoor scene understanding, 3D object detection has been extensively studied, and the accuracy on indoor point cloud data has been substantially improved. However, existing researches have been conducted on limited datasets, where the training and testing sets share the same distribution. In this paper, we consider the task of adapting indoor 3D object detectors from one dataset to another, presenting a comprehensive benchmark with ScanNet, SUN RGB-D and 3D Front datasets, as well as our newly proposed large-scale datasets ProcTHOR-OD and ProcFront generated by a 3D simulator. Since indoor point cloud datasets are collected and constructed in different ways, the object detectors are likely to overfit to specific factors within each dataset, such

as point cloud quality, bounding box layout and instance features. We conduct experiments across datasets on different adaptation scenarios including synthetic-to-real adaptation, point cloud quality adaptation, layout adaptation and instance adaptation, analyzing the impact of different domain gaps on 3D object detectors. We also introduce several approaches to improve adaptation performances, providing baselines for domain adaptive indoor 3D object detection, hoping that future works may propose detectors with stronger generalization ability across domains. Our benchmark datasets and baseline code can be found in: <https://github.com/JeremyZhao1998/DAVoteNet-release>.

CCS CONCEPTS

• Computing methodologies → Object detection; Scene understanding.

KEYWORDS

Domain Adaptation, Point Cloud Object Detection

ACM Reference Format:

Zijing Zhao, Zhu Xu, Qingchao Chen, Yuxin Peng, and Yang Liu. 2025. Investigating Domain Gaps for Indoor 3D Object Detection. In *Proceedings of the 33rd ACM International Conference on Multimedia (MM '25)*, October 27–31, 2025, Dublin, Ireland. ACM, New York, NY, USA, 7 pages. <https://doi.org/10.1145/3746027.3758275>

*Corresponding author

Permission to make digital or hard copies of all or part of this work for personal or classroom use is granted without fee provided that copies are not made or distributed for profit or commercial advantage and that copies bear this notice and the full citation on the first page. Copyrights for components of this work owned by others than the author(s) must be honored. Abstracting with credit is permitted. To copy otherwise, or republish, to post on servers or to redistribute to lists, requires prior specific permission and/or a fee. Request permissions from permissions@acm.org.

MM '25, October 27–31, 2025, Dublin, Ireland

© 2025 Copyright held by the owner/author(s). Publication rights licensed to ACM. ACM ISBN 979-8-4007-2035-2/2025/10...\$15.00
<https://doi.org/10.1145/3746027.3758275>

1 INTRODUCTION

As a fundamental task for 3D perception and indoor scene understanding, indoor 3D object detection has been extensively studied. Most 3D object detectors for indoor scenes are designed for point cloud data due to its adaptability, precision, and richness of information. Indoor 3D detectors [12, 13, 15] have achieved remarkable success in identifying and localizing objects in point clouds.

Though achieving great progress, existing indoor 3D object detection researches are mainly conducted on ScanNet dataset [4] and SUN RGB-D dataset [17]. Detectors are trained and evaluated within each dataset where the training and testing set share the same data distribution. As illustrated in fig. 1(a), point clouds in ScanNet dataset are constructed by thorough scans of RGB-D videos, thus with higher quality but relatively fewer scenes. Point clouds in SUN RGB-D dataset are converted through single RGB-D images, exhibiting large areas of point omission. In practical applications, detectors trained on data from a specific domain may need to generalize to deployment environments with distributional shift, i.e. domain adaptation problem which has rarely been explored in indoor 3D object detection field.

Domain adaptation for point cloud data has been studied on object classification task [2, 14, 16], outdoor LiDAR detection task [3, 11, 20] and indoor semantic segmentation task [6]. However, object detection on indoor point clouds has the following challenges: (1) Compared with 3D instance classification and outdoor LiDAR detection task, indoor scene point clouds can be constructed through multiple ways, creating more aspects of domain gap factors with larger domain gap to be solved. (2) Compared with outdoor LiDAR detection, indoor 3D detection requires to distinguish multiple object categories (more than 10 categories v.s. only detecting cars) with higher object diversity, resulting in richer semantics to be learned and adapted. (3) Localizing objects in indoor 3D scenes faces the challenges of close proximity of objects, sometimes even overlapping bounding boxes (e.g. a chair placed under a table), which may not appear in classification, segmentation and outdoor LiDAR detection tasks.

Only a few studies (e.g., [23]) have explored domain adaptation techniques for indoor 3D object detection, while their focus has been limited to the synthetic-to-real adaptation scenario. However, indoor 3D object detection encompasses a broader range of domain variations and practical application scenarios, which are not adequately represented or evaluated by current benchmarks. To facilitate a more systematic investigation of the various sources of domain shift that affect the performance of indoor 3D object detectors, we introduce a suite of comprehensive benchmarks. These benchmarks are constructed from both widely used public datasets and newly developed datasets designed to capture diverse conditions.

As shown in fig. 1(a), we construct our benchmarks using five representative indoor scene datasets. ScanNet [4] represents high-quality real-world point clouds acquired through dense scanning. SUN RGB-D [17] also contains real scenes but is captured with a single RGB-D image per scene, resulting in sparse and incomplete point clouds. 3D Front [8] provides synthetic indoor layouts with detailed 3D furniture models, but its scale is limited due to manual layout design by human experts. We further introduce two new

datasets: ProcTHOR-OD and ProcFront. We programmatically generates layouts and places synthetic objects by a simulator platform to produce ProcTHOR-OD, enabling large-scale and diverse scene generation. ProcFront uses the same layouts as ProcTHOR-OD but integrates instances from 3D Front, allowing controlled analysis of layout and instance domain gaps.

After selecting a consistent subset of instance categories across datasets, we combine the five datasets to construct a suite of domain adaptation benchmarks, covering the following scenarios: (1) Synthetic-to-real adaptation: Following [23], we evaluate 3D Front → ScanNet and 3D Front → SUN RGB-D, and additionally propose ProcTHOR-OD → ScanNet as a new synthetic-to-real setting where the source domain has larger data scale. (2) Point cloud quality adaptation: We test ScanNet → SUN RGB-D to assess the performance drop when transferring from high-quality scans to lower-quality, single-frame point clouds. (3) Layout adaptation: To isolate the impact of layout differences, we evaluate ProcFront → 3D Front. The two datasets share the same instance models but differ in scene layouts. (4) Instance adaptation: To examine domain gaps at the instance level, we evaluate ProcTHOR-OD → ProcFront, where the layouts remain the same but object appearances vary.

Under such benchmarks, we conduct experiments on the commonly used VoteNet [13] detector. As shown in fig. 1(b), the detector performs well within each dataset (blue bars, trained and evaluated within target dataset), but cross-dataset evaluation shows a significant performance drop (orange bars, trained by source and evaluated on target dataset). We also implement several commonly used domain adaptation approaches in other tasks to improve adaptation performances. These approaches serve as baselines for domain adaptive indoor 3D object detection, hoping that future works may propose detectors or frameworks with stronger generalization ability across domains. Our benchmark datasets and baseline code can be found in: <https://github.com/JeremyZhao1998/DAVoteNet-release>.

We summarize the main contributions of this paper as follows:

- We introduce two new datasets, ProcTHOR-OD and ProcFront which are automatically generated in simulation, offering high scalability and controllability, and are well-suited for studying domain adaptation for indoor 3D object detection.
- We propose a comprehensive suite of benchmarks by combining ScanNet, SUN RGB-D, 3D Front, and our newly proposed datasets to isolate and evaluate key domain gap factors, including synthetic-to-real shifts, point cloud quality, layout variations, and instance-level differences.
- We implement and evaluate several domain adaptation strategies for indoor 3D object detection, providing strong baselines for future research.

2 RELATED WORKS

2.1 Indoor point cloud datasets

As a universal 3D structure representation, point cloud data has been widely used in 3D indoor scene understanding tasks. Various 3D indoor scene datasets [1, 4, 17] have been proposed by multiple construction ways. SUN RGB-D dataset [17] converts single RGB-D images into 3D point clouds. ScanNet dataset [4] collects RGB-D videos through large amount of indoor rooms with rich semantic annotations, and has been the most widely used dataset in indoor

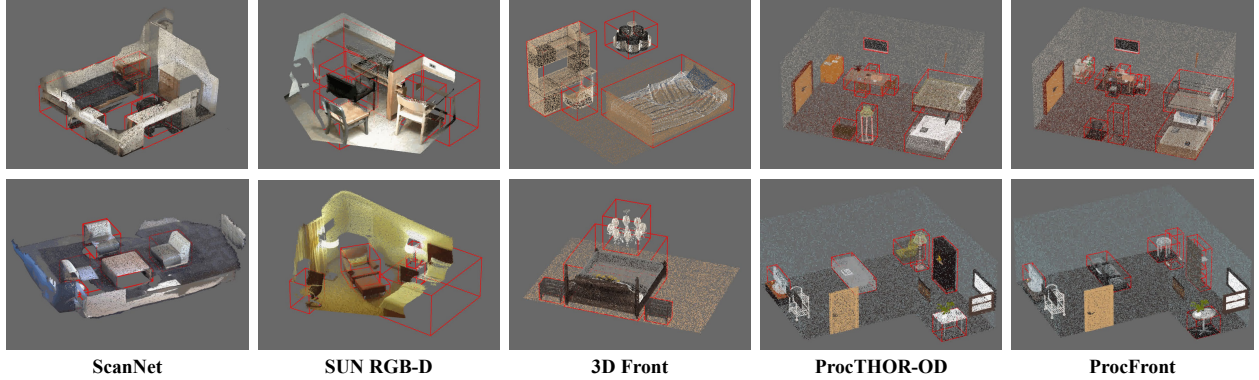


Figure 2: Visualization for typical scenes in the selected datasets of our proposed benchmarks.

3D object detection and semantic segmentation task. Simulated datasets like Structured3D [25] and 3D Front [8] are proposed to accomplish large-scale training with relatively low cost. However, these datasets are created by human designers and thus still have high construction cost. ProcTHOR [5] offers an indoor scene generation framework with a fully simulated dataset which mainly focus on embodied AI tasks such as navigation.

Despite their contributions to downstream tasks, existing datasets and benchmarks remain limited in scale, quality, and label diversity. They also assume identical distributions between training and testing sets, whereas this paper focuses on cross-domain adaptation for indoor 3D object detection. To this end, we introduce the ProcTHOR-OD and ProcFront datasets using the AI2-THOR platform [5], and combine them with existing datasets to establish new domain adaptation benchmarks.

2.2 Indoor 3D object detection on Point Clouds

Indoor 3D object detection is a fundamental task in indoor scene understanding, serving as the upstream task for 3D visual grounding, question answering and navigation. 3D-SIS [9] back projects the 2D feature vector onto the associated voxel in the 3D grid to achieve 3D detection and segmentation. VoteNet by [13] adopt deep hough voting strategy to train the model to group points for detection proposal generation. In recent years, transformer architectures are also introduced to detect objects in point clouds [15, 21, 26]. V-DETR [15] equips the detection transformer with 3D Vertex Relative Position Encoding which computes each point's encoding relative to the box vertices predicted by queries to enforce locality.

Though achieving great success, these studies all focus on performances where the training and testing set share the same data distribution. The domain adaptation ability of indoor 3D object detectors has not yet been explored. In this paper, we mainly conduct experiments on VoteNet [13] due to its popular use among indoor scene understanding tasks and its lightweight architecture.

2.3 Domain adaptation for point clouds

Prior work on 3D domain adaptation has primarily focused on classification, segmentation, and LiDAR-based detection tasks. PointDA [14] first introduced a domain adaptation method for 3D object classification by reconstructing local point features. Subsequent studies

[2, 16] proposed global feature reconstruction and self-training strategies to improve adaptation performance. For semantic segmentation, [6] explored synthetic-to-real adaptation via data augmentation and mixing.

LiDAR-based detection in autonomous driving scenes has a close relationship with indoor point cloud object detection. The pioneer work [20] evaluate cross-dataset performance of LiDAR detectors, followed by multiple techniques [3, 10, 11] that enhance domain adaptation performance by self-training, point completion, and pseudo-label refinement. Nonetheless, adapting to indoor 3D detection poses distinct challenges: (1) unlike autonomous driving datasets where all point clouds are LiDAR-generated, indoor point clouds arise from diverse sources, leading to more complex and varied domain gaps; (2) LiDAR point cloud detection typically focuses on a single object category (e.g., cars), whereas indoor detection involves a wider range of object classes (more than 10) with richer semantics. In this paper, we investigate the domain gaps for indoor 3D object detection task, providing the first comprehensive benchmark and several baselines.

3 DATASETS AND BENCHMARKS

To build the domain adaptation benchmarks for indoor 3D object detection, in this section, we review existing indoor 3D object detection datasets in section 3.1 and introduce our newly proposed datasets ProcTHOR-OD and ProcFront in section 3.2. We then analyze the differences of datasets in multiple aspects, and introduce our proposed domain adaptation benchmarks in section 3.3.

3.1 Existing indoor 3D object detection datasets

Existing indoor 3D object detection approaches are primarily evaluated on ScanNet [4] and SUN RGB-D [17] datasets. 3D Front [8] is also introduced as a synthetic dataset for indoor point cloud detection. ScanNet [4] is one of the most widely used datasets for indoor 3D scene understanding, consisting of 2.5M RGB-D video frames from real-world rooms, reconstructed into CAD models and converted into point clouds. As shown in fig. 2, scenes in ScanNet dataset are fully scanned thus has a relatively high quality. The standard split includes 1,201 training scenes and 312 testing scenes, with annotations for 529 object categories. SUN RGB-D [17] comprises 10,335 single-frame RGB-D images collected from four different

Table 1: Scale statistics of different datasets

Dataset	Point cloud source	Train / val	Object annotation
SUN RGB-D [17]	Single RGB-D images	5,073 / 4,828	54,376
ScanNet [4]	RGB-D videos	1,201 / 312	29,035
3D Front [8]	Synthetic meshes	5,080 / 370	31,022
ProcTHOR-OD	Synthetic meshes	8,000 / 2,000	238,003
ProcFront	Synthetic meshes	8,000 / 2,000	238,003

sensors. It offers tools for point cloud generation and includes 5,073 training scenes and 4,828 test scenes, annotated with 620 object categories for 3D detection and orientation estimation. As shown in fig. 2, SUN RGB-D scenes have obvious point omission areas. 3D Front [8] contains over 6,800 synthetic indoor scenes with detailed 3D furniture models and designer-created layouts. It provides mesh models and point cloud generation tools via rendering and depth fusion, with 5,080 scenes for training and 370 for testing in semantic segmentation and layout tasks. As shown in fig. 2, 3D Front scenes have uniformly sampled high-quality 3D point clouds.

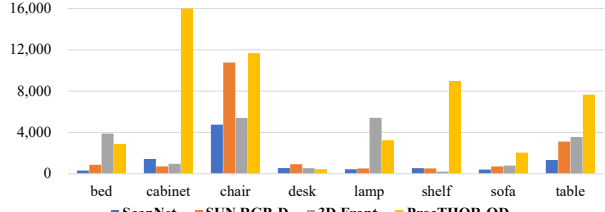
The scale of indoor 3D datasets is often constrained by the substantial human effort required for data collection and calibration. Manually annotated datasets also inevitably suffer from label noise [22]. As a synthetic dataset, 3D Front alleviates the burden of data collection. However, it still relies on expert-designed room configurations, which limits its scalability. Furthermore, existing datasets lack extensibility and are insufficient for systematically investigating the various types of domain gaps that may arise in real-world applications.

3.2 Our proposed ProcTHOR-OD and ProcFront

To address the data scale issue, researches have tried to use simulators to create large-scale datasets with precise annotations at a low cost such [8, 25]. However, the human designed indoor scenes still faces the high cost of construction and can hardly be scaled up.

To address the scarcity of synthetic indoor 3D object detection datasets and to enable controlled analysis of domain gap factors, we construct fully synthetic datasets using the AI2-THOR simulation platform. Following the ProcTHOR pipeline [5], we randomly generate large-scale, diverse single-room layouts through a multi-stage process, including room specification, floorplan generation, and the placement of structural elements, large objects, wall-mounted items, and surface objects. This procedure yields accurate object and structure information without manual annotation. The generated layouts are exported in mesh format (e.g., .glb), preserving geometry and surface details, from which we uniformly sample points to construct point clouds. We generate 10,000 scenes and randomly split 8,000 for training set and 2,000 for evaluation. Our ProcTHOR-OD dataset differs from prothor-10k [5] in two key ways: (1) We generate single-room layouts instead of multi-room scenes to better suit 3D object detection instead of robotic navigation. (2) Unlike prothor-10k, which mainly uses 2D images and floorplan configuration, we export 3D meshes and sample point clouds to support point-based learning.

Through the benefit of scalability and extensibility, we are able to control the layout and object instances in the generated scenes to isolate the domain gap factors for a better analysis. We construct

**Figure 3: Instance count by category across datasets.**

ProcFront, a novel intermediate domain bridging ProcTHOR-OD and 3D Front, by combining the large-scale scene layouts from ProcTHOR-OD with fine-grained, category-specific 3D object models curated from the 3D Front dataset. Specifically, with the determined object layout of ProcTHOR-OD and known instance information of 3D Front, we randomly retrieve instances in 3D Front scenes within a range of similar length, width and height. For an instance with similar size, we place it into the original bounding box after size scaling and rotation to align the new instance with original bounding box, ensuring the correctness of annotations in the new dataset. In this way, ProcFront share the same layout distribution with ProcTHOR and the very similar instance distribution with 3D Front to facilitate isolated analysis of domain gap factors. The scene number of both ProcTHOR-OD and ProcFront is more than 5 times larger than ScanNet, and the number of bounding box annotations is an order of magnitude larger than ScanNet and SUN RGB-D.

3.3 Domain adaptation benchmarks

3.3.1 Analysis of dataset status. In fig. 2 we present typical scenes of each dataset. In table 1 and fig. 3 we show the statistical information of the datasets. We analyze the differences of these datasets as follows: (1) *Data scale*: As shown in table 1, while existing real-world datasets are limited in scale and annotation quality, our proposed synthetic datasets offer low-cost, high-precision annotations with 10k scenes and 238k bounding boxes—an order of magnitude more than their real-world counterparts. (2) *Style(synthetic to real)*: As illustrated in fig. 2, the style difference exists between synthetic and real-world datasets. Though providing high quality point clouds, synthetic datasets lack the texture details and material realism of objects in real-world environments. (3) *Point cloud quality*: As can be visualized in fig. 2, thoroughly scanned ScanNet dataset have high quality while SUN RGB-D point clouds exhibit obvious point omission. The synthetic datasets have high quality point clouds without the problem of scan omission. (4) *Room layout*: As shown in table 1, ScanNet and SUN RGB-D are collected from real-world indoor environments, featuring naturally cluttered object arrangements, whereas 3D Front consists of expert-designed scenes with clean and organized layouts. In contrast, our proposed ProcTHOR dataset adopts automatically generated layouts, which differ from human-designed ones in style but offer significantly greater scale and diversity. (5) *Instance features*: Different datasets exhibit distinct instance-level characteristics, even within the same object category. As shown in fig. 2, objects such as beds can vary significantly in appearance. Moreover, as illustrated in fig. 3, the distribution of instance counts also differs notably, with our synthetic dataset providing a substantially larger number of instances.

Table 2: Cross domain mAP on ProcTHOR-OD → ScanNet

Method	bed	cabinet	chair	desk	lamp	shelf	sofa	table	mAP
source	23.33	0.46	41.45	6.90	1.68	2.99	44.44	30.11	18.92
target	77.69	22.41	64.91	55.81	12.68	19.59	71.79	45.62	46.31

Table 3: Cross domain mAP on 3D Front → ScanNet

Method	bed	bk.shf	cabnt	chair	desk	lamp	n.stnd	shelf	sofa	tab	mAP
source	12.73	12.65	0.78	38.92	6.82	0.55	1.01	1.03	35.93	15.38	12.58
target	77.21	36.68	21.63	65.96	57.22	12.70	62.17	23.58	73.57	50.12	48.08

Table 4: Cross domain mAP on 3D Front → SUN RGB-D

Method	bed	bk.shf	cabnt	chair	desk	lamp	n.stnd	shelf	sofa	tab	mAP
source	31.87	1.52	0.20	25.20	4.91	0.17	0.24	0.12	13.14	21.29	9.87
target	85.33	33.74	8.52	71.54	26.94	32.00	65.29	12.87	65.70	53.33	45.52

3.3.2 Domain adaptation scenarios. Based on the analysis of differences between datasets, we propose 4 domain adaptation settings including totally 6 sets of evaluation benchmarks based on the practical requirements:

Synthetic to real adaptation: Fully leveraging the large-scale, high-quality synthetic data, the detectors should be capable of adapting to real-world scenarios to meet practical requirements. Under this setting, we use our proposed ProcTHOR-OD as source domain and ScanNet as target domain. Following [23], we also evaluate 3D Front → ScanNet and 3D Front → SUN RGB-D.

Point cloud quality adaptation: Detectors trained on thoroughly scanned datasets should be able to adapt to environments where the point clouds are of lower quality. Under this setting, we use ScanNet as source domain and SUN RGB-D as target domain.

Layout adaptation: Instance placement layout is a core feature of a 3D scene in detection task. By rule-based framework, our proposed ProcFront has large scale diverse layout and at the same time shares the same instances with 3D Front. We use ProcFront as source domain and 3D Front as target domain, hoping the detector to generalize from generated layout to manually designed layout.

Instance adaptation: To evaluate instance-level generalization ability of detectors, we control the layout by ProcTHOR-OD and ProcFront, only studying the instance difference. We use ProcTHOR-OD as source domain and ProcFront which contains additional instances as target domain.

For each domain-adaptation benchmark, we retain only the categories shared by the source and target datasets, excluding structural objects (e.g., windows, doors, pictures) and very small objects (e.g., phones, eggs, knives). The resulting category sets for each benchmark are listed in the tables in section 4.2.

4 EXPERIMENTS AND ANALYSIS

4.1 Setup and details

In our experiments, we apply commonly used indoor 3D object detector VoteNet [13] to evaluate the cross domain performance

Table 5: Cross domain mAP on ScanNet → SUN RGB-D

Method	bed	bk.shf	cbnt	chr	desk	gbg.c	lamp	nstd	shf	sink	sofa	tab	tlt	tv	mAP
source	58.7	12.3	1.9	38.5	11.7	15.4	7.6	20.1	6.5	16.5	42.3	32.9	56.8	8.5	23.6
target	82.1	28.7	8.3	71.5	24.7	43.9	33.0	62.2	13.5	51.2	63.8	50.6	86.2	20.0	45.7

Table 6: Cross domain mAP on ProcFront → 3D Front

Method	bed	cabnt	chair	desk	lamp	shelf	sofa	tab	tv.stnd	mAP
source	95.53	0.87	59.54	15.45	0.28	0.34	41.86	38.80	21.11	30.42
target	99.99	74.73	97.70	83.03	95.52	72.52	99.27	92.28	0.63	79.52

Table 7: Cross domain mAP on ProcTHOR-OD → ProcFront

Method	bed	cabnt	chair	desk	lamp	shelf	sofa	tab	tv.stnd	mAP
source	33.13	0.23	42.35	3.59	3.76	2.56	63.28	46.11	38.22	25.92
target	85.59	21.32	65.26	56.23	35.99	10.58	87.13	73.37	56.68	54.68

and domain adaptation approaches. We randomly sample 40,000 points per scene for training. In addition to XYZ coordinates, we include height feature and RGB color feature for each point. We train the network end-to-end with AdamW optimizer and batch size 32 for 90 epochs. The initial learning rate is 0.008, and is decreased by 10× after 65 and 80 epochs.

During inference, we post-process the proposals with dropping empty boxes (less than 5 points in a box), dropping too little boxes (boxes with side length less than 0.001 m) and 3D NMS (non-maximum suppression) with IoU threshold of 0.25. We report the evaluation metric of mAP (mean average precision) following the protocol of [18] with IoU threshold 0.25. More details can be found in our link of benchmark datasets and code.

4.2 Analysis of domain gaps

We present the basic experimental results on our proposed benchmarks in table 2 to 7 and further domain adaptation results in table 8 to analysis the impact of multiple domain gap factors mentioned in section 3.3.1.

Style(synthetic to real): ProcTHOR-OD → ScanNet, 3D Front → ScanNet and 3D Front → SUN RGB-D exhibit synthetic to real style gap, as illustrated in table 2, table 3 and table 4. ScanNet trained detector performs well on its own evaluation set, but drastically decline to only 12.58 mAP when trained on 3D Front. The result on ProcTHOR trained model is slightly better (18.92 mAP), illustrating that data scale contributes to performance even when domain gap is rather large. SUN RGB-D trained detector has 45.52 mAP within its domain, but declines to only 9.87 mAP when trained on synthetic dataset. The SUN RGB-D serve as a more challenging target domain dataset, given the low quality point cloud that is converted from single RGB-D images. Experiments shows that synthetic-to-real gap is a challenging hurdle for domain adaptive indoor 3D object detection among our proposed benchmarks.

Point cloud quality: The ScanNet → SUN RGB-D benchmark isolates the point-cloud quality gap: adapting between two real datasets avoids confounds from instance shape and texture. As

Table 8: Baseline results on our proposed benchmarks

Method	proc2scan	front2scan	front2sun	scan2sun	pf2front	proc2pf
Source	18.90	12.58	9.87	23.56	30.42	25.92
Size	18.92	13.53	9.92	25.56	28.83	25.30
Prior 10 shots	17.47	14.05	10.39	24.05	32.56	27.00
100 shots	33.86	25.83	10.54	24.58	37.01	29.23
VSS [6]	20.31	16.72	10.61	25.26	28.06	24.32
UDA MT [19]	20.43	15.03	10.32	25.25	31.77	27.43
RV [7]	20.89	15.27	10.40	24.92	32.45	28.50
Oracle	46.31	48.08	45.53	45.70	79.52	54.68

shown in table 5, a model trained on ScanNet attains 23.56 mAP on SUN RGB-D—well below the 45.70 mAP within domain—highlighting the risk of deploying models trained on well-scanned data to lower-quality point clouds and the value of this benchmark.

Layout adaptation: As shown in Table 6, the flexibility of our generative data framework lets us isolate the effect of the layout domain gap. Although ProcFront uses the same instance models as 3D-Front, switching from automatically generated layouts to human-designed ones sharply reduces performance—from 93.81 to 22.62 mAP. This highlights scene layout as a major driver of domain shift in object detection.

Instance adaptation: As the fundamental task of object detection, the performance not only requires localization, but also recognition of instances. In table 7 we control the layout as the same and evaluate the impact of instance change. Results shows that even with exactly the same layout, instance feature gap also cause a decline in performance, from 73.28 to 25.64 mAP.

4.3 Domain adaptation approaches

As shown in table 8, we introduce several domain adaptation approaches including methods using target domain priors (block “Prior” in the table) and unsupervised domain adaptation techniques (block “UDA” in the table) to improve adaptation performance, presenting a first series of baselines for this problem.

4.3.1 Using target domain priors. When the domain gap is substantial, lightweight target-domain priors—far easier to obtain than exhaustive target annotations—can significantly boost cross-domain detection performance. In the “Prior” block of table 8, we report results for different types of priors.

Using object size prior: Different datasets exhibit average object size difference. By simply adopting the target domain statistical prior of mean sizes for each category instead of precise labels, reported in line “Size”, the detector shows performance gains in most benchmarks where the source and target domains have a larger instance gap. (In “pf2front” and “proc2pf” where the source and target domains share a large number of instances, the size prior seems to have no effect.) This observation shed a light on future studies to estimate target domain object sizes.

Few-shot fine-tuning: In line “10 shots” and “100 shots” we report the result of fine-tuning the source-only trained model with 10 and 100 labeled target scenes. On all the baselines, 10-shot fine-tuning improves the performance only slightly relative to the

source-only baseline. Using 100 target domain annotated scenes yields substantial performance gains. However, performance still lags far behind the target-domain oracle. Given the high cost of collecting and annotating real-world target scenes, unsupervised domain adaptation remains a highly desirable direction.

4.3.2 Unsupervised Domain Adaptation. Unsupervised domain adaptation setting requires only the point clouds without the need of annotation. We evaluate different domain adaptation techniques on our proposed benchmarks, including virtual scan simulation [6] (reported in line “VSS”), mean teacher (reported in line “MT”) [19], and reliable voting [7] (reported in line “RV”). Note that due to the difference on task setting, we re-implement all the methods and make minor adjustments for object detection task.

Virtual scan simulation. Introduced by DODA [6] for domain-adaptive indoor point cloud segmentation, Virtual Scan Simulation (VSS) targets the synthetic-to-real gap by mimicking imperfections in real reconstructions. VSS models (i) sensor noise, perturbing each point’s (x, y, z) coordinates, and (ii) view occlusion, removing occluded points via multi-view projection.

Mean teacher. Originally proposed for semi-supervised learning [19] and now widely used for UDA across classification, detection, and segmentation on both 2D images [24] and 3D LiDAR point clouds [3], the mean-teacher framework trains a source-only model and initializes a teacher that generates pseudo-labels for target samples to supervise a student; the teacher is typically updated from the student (e.g., via EMA) to enforce consistency.

Reliable voting. Proposed for domain-adaptive point cloud classification [7], reliable voting improves pseudo label selection in the mean-teacher framework. In our implementation, we cache features and predicted categories for all source-domain instance proposals; during training, for each target proposal we retrieve its top- K most similar source proposals and check whether their categories agree with the target prediction. We accept the target pseudo-label only when this cross-domain vote is reliable.

As shown in the “UDA” block of table 8, VSS augmentation performs well in synthetic-to-real settings but lacks generality for layout and instance adaptation. (The augmented data has lower point cloud quality, thus harms the performance where the target domain has high-quality point clouds in “pf2front” and “proc2pf”.) The mean-teacher approach consistently works across all baselines, demonstrating its generality, and reliable voting (RV) consistently improves mean-teacher results, indicating the effectiveness of pseudo-label filtering. More details can be seen in our baseline code link.

5 CONCLUSION

In this paper, we conduct a comprehensive analysis of domain gaps across indoor 3D object detection datasets. By combining three widely used datasets: ScanNet, SUN RGB-D, and 3D-Front, with our two newly proposed datasets, ProcTHOR-OD and ProcFront, we build the first comprehensive benchmark suite for domain adaptive indoor 3D object detection. This suite comprises six benchmarks spanning four adaptation scenarios: synthetic-to-real, point cloud quality, layout, and instance adaptation. We introduce several baseline methods and evaluate them on our benchmarks, highlighting future directions for improving adaptation performance.

ACKNOWLEDGMENTS

This work was supported by the grants from the National Natural Science Foundation of China (62372014, 62525201, 62132001, 62432001), Beijing Nova Program and Beijing Natural Science Foundation (4252040, L247006).

REFERENCES

- [1] Iro Armeni, Ozan Sener, Amir R Zamir, Helen Jiang, Ioannis Brilakis, Martin Fischer, and Silvio Savarese. 2016. 3d semantic parsing of large-scale indoor spaces. In *Proceedings of the IEEE conference on computer vision and pattern recognition*. 1534–1543.
- [2] Adriano Cardace, Riccardo Spezialetti, Pierluigi Zama Ramirez, Samuele Salti, and Luigi Di Stefano. 2023. Self-Distillation for Unsupervised 3D Domain Adaptation. In *Proceedings of the IEEE/CVF Winter Conference on Applications of Computer Vision (WACV)*.
- [3] Gyusam Chang, Wonseok Roh, Sujin Jang, Dongwook Lee, Daehyun Ji, Gyeongrok Oh, Jinsun Park, Jinkyu Kim, and Sangpil Kim. 2024. Cmda: Cross-modal and domain adversarial adaptation for lidar-based 3d object detection. In *Proceedings of the AAAI Conference on Artificial Intelligence*, Vol. 38. 972–980.
- [4] Angela Dai, Angel X Chang, Manolis Savva, Maciej Halber, Thomas Funkhouser, and Matthias Nießner. 2017. Scannet: Richly-annotated 3d reconstructions of indoor scenes. In *Proceedings of the IEEE conference on computer vision and pattern recognition*. 5828–5839.
- [5] Matt Deitke, Eli VanderBilt, Alvaro Herrasti, Luca Weihs, Kiana Ehsani, Jordi Salvador, Winson Han, Eric Kolve, Aniruddha Kembhavi, and Roozbeh Mottaghi. 2022. ProcTHOR: Large-Scale Embodied AI Using Procedural Generation. *Advances in Neural Information Processing Systems* 35 (2022), 5982–5994.
- [6] Runyu Ding, Jihua Yang, Li Jiang, and Xiaojian Qi. 2022. Doda: Data-oriented sim-to-real domain adaptation for 3d semantic segmentation. In *European Conference on Computer Vision*. Springer, 284–303.
- [7] Hehe Fan, Xiaojun Chang, Wanyue Zhang, Yi Cheng, Ying Sun, and Mohan Kankanhalli. 2022. Self-Supervised Global-Local Structure Modeling for Point Cloud Domain Adaptation With Reliable Voted Pseudo Labels. In *Proceedings of the IEEE/CVF Conference on Computer Vision and Pattern Recognition (CVPR)*. 6377–6386.
- [8] Huan Fu, Bowen Cai, Lin Gao, Ling-Xiao Zhang, Jiaming Wang, Cao Li, Qixun Zeng, Chengyue Sun, Rongfei Jia, Binqiang Zhao, et al. 2021. 3d-front: 3d furnished rooms with layouts and semantics. In *Proceedings of the IEEE/CVF International Conference on Computer Vision*. 10933–10942.
- [9] Ji Hou, Angela Dai, and Matthias Nießner. 2019. 3d-sis: 3d semantic instance segmentation of rgb-d scans. In *Proceedings of the IEEE/CVF conference on computer vision and pattern recognition*. 4421–4430.
- [10] Qianjiang Hu, Daizong Liu, and Wei Hu. 2023. Density-insensitive unsupervised domain adaption on 3d object detection. In *Proceedings of the IEEE/CVF Conference on Computer Vision and Pattern Recognition*. 17556–17566.
- [11] Jiaming Liu, Rongyu Zhang, Xiaochi Li, Xiaowei Chi, Zehui Chen, Ming Lu, Yangdong Guo, and Shanghang Zhang. 2024. BEVUDA: Multi-geometric space alignments for domain adaptive BEV 3D object detection. In *2024 IEEE International Conference on Robotics and Automation (ICRA)*. IEEE, 9487–9494.
- [12] Xuran Pan, Zhuofan Xia, Shiji Song, Li Erran Li, and Gao Huang. 2021. 3d object detection with pointformer. In *Proceedings of the IEEE/CVF Conference on Computer Vision and Pattern Recognition*. 7463–7472.
- [13] Charles R Qi, Or Litany, Kaiming He, and Leonidas J Guibas. 2019. Deep hough voting for 3d object detection in point clouds. In *proceedings of the IEEE/CVF International Conference on Computer Vision*. 9277–9286.
- [14] Can Qin, Haoxuan You, Lichen Wang, C-C Jay Kuo, and Yun Fu. 2019. Pointdan: A multi-scale 3d domain adaption network for point cloud representation. *Advances in Neural Information Processing Systems* 32 (2019).
- [15] Yichao Shen, Zigang Geng, Yuhui Yuan, Yutong Lin, Ze Liu, Chunyu Wang, Han Hu, Nanning Zheng, and Baining Guo. 2023. V-DETR: DETR with Vertex Relative Position Encoding for 3D Object Detection. *arXiv:2308.04409* [cs.CV]
- [16] Yuefan Shen, Yanchao Yang, Mi Yan, He Wang, Youyi Zheng, and Leonidas J. Guibas. 2022. Domain Adaptation on Point Clouds via Geometry-Aware Implicits. In *Proceedings of the IEEE/CVF Conference on Computer Vision and Pattern Recognition (CVPR)*. 7223–7232.
- [17] Shuran Song, Samuel P Lichtenberg, and Jianxiong Xiao. 2015. Sun rgb-d: A rgb-d scene understanding benchmark suite. In *Proceedings of the IEEE conference on computer vision and pattern recognition*. 567–576.
- [18] Shuran Song and Jianxiong Xiao. 2016. Deep sliding shapes for amodal 3d object detection in rgb-d images. In *Proceedings of the IEEE conference on computer vision and pattern recognition*. 808–816.
- [19] Antti Tarvainen and Harri Valpola. 2017. Mean teachers are better role models: Weight-averaged consistency targets improve semi-supervised deep learning results. *Advances in neural information processing systems* 30 (2017).
- [20] Yan Wang, Xiangyu Chen, Yurong You, Li Erran Li, Bharath Hariharan, Mark Campbell, Kilian Q Weinberger, and Wei-Lun Chao. 2020. Train in germany, test in the usa: Making 3d object detectors generalize. In *Proceedings of the IEEE/CVF Conference on Computer Vision and Pattern Recognition*. 11713–11723.
- [21] Yu-Qi Yang, Yu-Xiao Guo, Jian-Yu Xiong, Yang Liu, Hao Pan, Peng-Shuai Wang, Xin Tong, and Baining Guo. 2025. Swin3d: A pretrained transformer backbone for 3d indoor scene understanding. *Computational Visual Media* 11, 1 (2025), 83–101.
- [22] Qingtao Yu, Heming Du, Chen Liu, and Xin Yu. 2024. When 3D Bounding-Box Meets SAM: Point Cloud Instance Segmentation with Weak-and-Noisy Supervision. In *Proceedings of the IEEE/CVF Winter Conference on Applications of Computer Vision*. 3719–3728.
- [23] Wang Yunsong, Na Zhao, and Gim Hee Lee. 2024. Syn-to-Real Unsupervised Domain Adaptation for Indoor 3D Object Detection. *arXiv:2406.11311* [cs.CV]
- [24] Zijing Zhao, Sitong Wei, Qingchao Chen, Dehui Li, Yifan Yang, Yuxin Peng, and Yang Liu. 2023. Masked retraining teacher-student framework for domain adaptive object detection. In *Proceedings of the IEEE/CVF International Conference on Computer Vision*. 19039–19049.
- [25] Jia Zheng, Junfei Zhang, Jing Li, Rui Tang, Shenghua Gao, and Zihan Zhou. 2020. Structured3d: A large photo-realistic dataset for structured 3d modeling. In *Computer Vision–ECCV 2020: 16th European Conference, Glasgow, UK, August 23–28, 2020, Proceedings, Part IX* 16. Springer, 519–535.
- [26] Yun Zhu, Le Hui, Yaqi Shen, and Jin Xie. 2024. Spgroup3d: Superpoint grouping network for indoor 3d object detection. In *Proceedings of the AAAI Conference on Artificial Intelligence*, Vol. 38. 7811–7819.